Comparison of a state of the art Si IGBT and next generation fast switching devices in a 4 kW boost converter

Anthon, Alexander; Zhang, Zhe; Andersen, Michael A. E.

Published in:
Proceedings of 2015 IEEE Energy Conversion Congress and Exposition

Link to article, DOI:
10.1109/ECCE.2015.7310080

Publication date:
2015

Document Version
Peer reviewed version

Comparison of a State of the Art Si IGBT and Next Generation Fast Switching Devices in a 4 kW Boost Converter

Alexander Anthon, Zhe Zhang, Michael A. E. Andersen
Dept. of Electrical Engineering
Technical University of Denmark
Kgs. Lyngby, Denmark
Email: jant@elektro.dtu.dk

***Abstract*—This paper gives a comprehensive comparison of two promising silicon carbide (SiC) switching devices, i.e. normally-off SiC MOSFET and a normally-on SiC JFET, as alternatives to a conventional state of the art Si IGBT. The comparison uses datasheet information to determine conduction losses, switching transition measurements for switching loss calculations and electrical power measurements in a boost converter. Using SiC switching devices, switching energies can be reduced by almost 70 % and the forward voltages of such devices are much lower compared to the IGBT which then reduce the conduction losses. This reduction in semiconductor losses can increase overall converter efficiencies up to 0.4 % at 20 kHz or enable high frequency operation up to 100 kHz which then reduces the size and weight of the inductor by more than 75 % while still achieving efficiencies over 98.3 %.**

***Index Terms*—Si IGBT, SiC MOSFET, SiC JFET, Efficiency, Boost converter**

I. Introduction

In residential photovoltaic (PV) systems, transformer-less topologies are favored due to the smaller size, weight, lower cost and higher efficiencies compared to their transformer-based alternatives [1]. However, a boost converter as a preregulator is then necessary in order to ensure a DC link voltage large enough to obtain the desired grid voltage. For three-phase PV systems, the DC link voltage is typically in the range of 700 V and can reach up to 1000 V. Thus, the semiconductor devices are typically chosen to have a breakdown voltage of 1200 V, which limits the choice mainly to Si IGBTs.

For power converters equipped with such semiconductor devices, however, the switching frequency usually becomes the limiting factor when it comes to high efficiency power conversion. Where a simple boost converter generally requires only one diode, one switching element and one inductor, the latter in this configuration usually becomes bulky, heavy and expensive due to the low switching frequency operation of the Si IGBT in order to maintain a reasonable small input current ripple. Interleaved boost converter (IBC) topologies can therefore be an attractive alternative due to the reduced input current ripple [2] which consequently improves the power quality and power-point tracking (MPPT) performance [3] with the trade-offs against other criteria such as additional components, increased complexity or unequal load sharing [4]. To furthermore improve the performance of the preregulator stage of the PV system, previous work has investigated the use of new semiconductor devices made of silicon carbide (SiC) material. With the commercialization of SiC diodes in 2001 [5], which have the particular benefit of having zero reverse recovery current, the positive impact of the new kind of semiconductor devices on switching loss reduction and reduced electromagnetic interference (EMI) has been reported for instance in [6], [7] and efficiency improvements of up to 0.8 % in a boost converter with SiC diodes were achieved in [3].

After the successful commercialization of SiC diodes, research interest has moved towards the utilization of SiC semiconductor switching devices in power converters as direct replacements for Si IGBTs and Si MOSFETs. Due to the higher electric field breakdown strength of SiC material, not only the on-resistance can be reduced compared to a Si MOSFET of an equivalent rating [8], but also the switching energies (in particular compared to IGBTs [9]). The benefits of SiC switching devices compared to Si based alternatives for various applications have been reported in previous work [10]–[15].

Among the various SiC switching alternatives to date, two main candidates can be pointed out and are hence intensively tested in this work: The normally-off SiC MOSFET and the normally-on SiC JFET. Although previous work clearly highlights the potentials of these two SiC switching devices, neither of them have fully become the new standard component in commercial products. Apart from the small availability through distribution channels, main issues are related to the (long-term) reliability, which is still ongoing research work [16]–[18].

The SiC MOSFET is claimed to have long-term reliability issues due to its thin oxide layer [19], [20], which is a major reason for not utilizing it in commercial products. In contrast, the depletion mode JFET does not have the reliability issue like the SiC MOSFET and shows a superior short circuit behavior [21], however its normally-on behavior is the main argument

978-1-4673-7151-3/15/$31.00

TABLE I
SEMICONDUCTORS USED

Device	I_C or I_D at 25 °C [A]	V_{GE} or V_{GS} [V]	C_{oss} [pF]
Si IGBT	30	± 20	75
SiC MOSFET	36	$-10/+25$	80
SiC JFET	35	$-19.5/+2$	102

for not using it as a direct replacement for Si devices. the normally-on characteristic is a crucial aspect when it comes to voltage source inverters (VSI) comprising of large DC link capacitors and additional protection may then be necessary [22]. Although the normally-on characteristic can be overcome with an in series placed low voltage Si MOSFET in cascode configuration (either conventional cascode [23] or direct driven cascode [24], [25]), this solution also adds complexity to the system. In a current source converter like the boost converter, however, the normally-on characteristic of the JFET is not a major drawback and a pure normally-on SiC could be an option in such application.

Although switching and conduction performance of these two SiC switching devices can be found in previous work, a direct performance comparison other than simple double pulse test measurements [26] is not known to the authors. This paper therefore gives a comprehensive comparison between these two promising SiC switching device technologies compared to a conventional Si IGBT of an equivalent rating. The comparison uses semiconductor loss models derived from datasheet parameters (conduction losses), measured switching transitions (switching losses) and efficiency measurements on a 4 kW boost converter under exactly the same operating conditions. Compared to a Si IGBT based converter as a reference, this work provides design guidelines when adopting the new kind of switching devices.

II. COMPARISON OF SI AND SIC SWITCHES

The devices used in this comparison are Infineon's third generation Si IGBT IKW15N120H3, Cree's SiC MOSFET C2M0080120D and Infineon's normally-on SiC JFET IJW120R070T1 with their main characteristics given in Table I. Since SiC switching devices are claimed to replace Si IGBTs in the future, their gate driver circuits are discussed in order to point out the differences and similarities because each switching device needs a specific gate driver circuit as different voltage levels on the gate are required.

A. Si IGBT gate driver

The gate driver circuit for the Si IGBT is used as a reference for comparison of the SiC MOSFET and SiC JFET; all gate driver constellations are shown in Fig. 1. Based on Table I, the IGBT can be switched on and off with $\pm 20\,\mathrm{V}$ as an absolute maximum rating. It is recommended in high speed high power applications to use negative voltages for turning off the IGBTs in order to increase the gap between the gate driver voltage and the threshold voltage of the semiconductor device. Else the risk for unwanted turn on may be increased either due

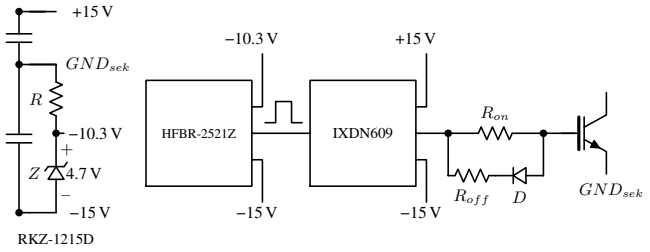

(a) Si IGBT

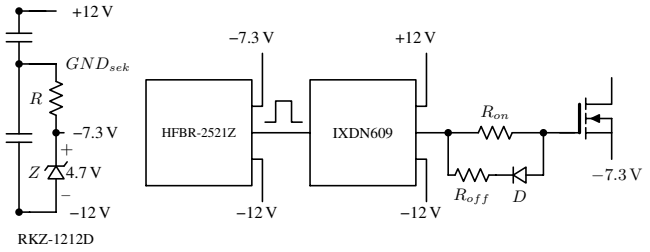

(b) SiC MOSFET

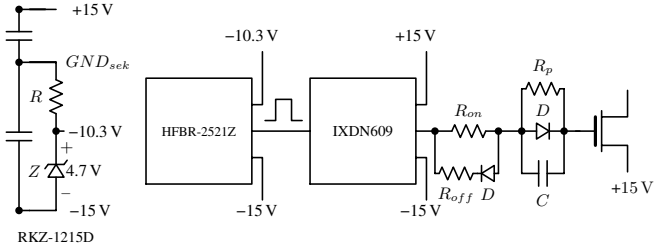

(c) SiC JFET

Fig. 1. Schematic of the gate driver circuits

to parasitic inductances in the switching loop or due to the effect of the Miller capacitance. For this reference design, only commercially available components are chosen to ease any reproduction. A 2 W DC/DC converter *RKZ-1215D* is used to provide galvanic isolation with $\pm 15\,\mathrm{V}$ output voltages which are used to turn the IGBT on and off, respectively. The signal transmission from the control board to the power stage is done with optic fiber, whose receiver *HFBR-2521Z* is driven with $4.7\,\mathrm{V}$ obtained by a simple zener diode. The PWM signal is amplified by the gate driver IC *IXDN609* supplied with $\pm 15\,\mathrm{V}$ yielding in a total voltage of 30 V. The collector of the IGBT is referenced to GND_{sek} which has been properly decoupled by two capacitors which are supposed to be placed as close as possible to the switching device in order to minimize any stray inductance in the gate driver loop.

B. SiC MOSFET gate driver

The absolut maximum ratings for the gate-source voltage of the SiC MOSFET are $-10\,\mathrm{V}$ for turn off and $+25\,\mathrm{V}$ for turn on. Hence the Si IGBT gate driver needs to be modified in order to fulfill these requirements. Taking into account some margin to stay safely within the absolute maximum ratings, the SiC MOSFET can be driven with approx. $-5\,\mathrm{V}$ and $+20\,\mathrm{V}$. Hence two things need to be modified:

1) Replace the DC/DC converter with the *RKZ-1212D* which provides galvanic isolation and two output voltages $\pm 12\,\mathrm{V}$
2) Reference the source of the SiC MOSFET to the voltage of the zener diode, i.e. $-7.3\,\mathrm{V}$

The driving voltage for turn on is then according to Kirchoff's voltage law (KVL)

$$V_{GSon} = +12\,\mathrm{V} - (-7.3\,\mathrm{V}) = 19.3\,\mathrm{V} \tag{1}$$

and the turn off voltage, respectively

$$V_{GSoff} = -12\,\mathrm{V} - (-7.3\,\mathrm{V}) = -4.7\,\mathrm{V} \tag{2}$$

Hence the SiC MOSFET can easily be adapted into a Si IGBT based converter with only minor modifications. Basically, only a change in the DC/DC converter and the reference voltage are necessary.

C. SiC JFET gate driver

The gate driver circuit for the SiC JFET requires more attention since the device differs internally from IGBTs or MOSFETs [27]. Since the JFET is a depletion mode device, it is turned on with a control voltage of $0\,\mathrm{V}$ and a negative voltage must be applied to turn the device off. The datasheet states this pinch-off voltage of the JFET to be around $-16\,\mathrm{V}$ which may vary from one device to another. Furthermore, at around $-23\,\mathrm{V}$, the gate-source junction enters reverse breakdown and hence a gate-source voltage of $-20\,\mathrm{V}$ is usually recommended in order to fully turn the device off. In [27], a driver circuit for a normally-on JFET is proposed to overcome this particular issue with the reverse breakdown, and it is therefore used in this work. Where the detailed explanation of the gate driver can be found in [27], it is only mentioned here that three additional electronic components are needed and the reference voltage, once again, must be shifted. The two modifications for the SiC JFET gate driver are therefore:

1) Place a RCD network between the gate resistance and the gate of the JFET
2) Reference the source of the JFET to the positive supply voltage of the DC/DC converter output, i.e. $+15\,\mathrm{V}$

D. Static characteristics

One of the properties of SiC based switching devices is to reduce the conduction losses. The voltage drop of a semiconductor device directly relates to the conduction losses which represent a significant contribution to the overall converter losses. The specific forward voltages for the devices used in this work are taken from datasheet information and are presented in Fig. 2. Once can see that over the whole current range of interest, the Si IGBT has the largest forward voltages. The reason for that is that the IGBT is a bipolar switching device which can be modeled as a series connection of a voltage source representing the zero on-state voltage V_0 and a dynamic resistance r_{on}. For a unipolar device such as the SiC MOSFET and the SiC JFET, there is no zero on-state voltage and only the channel resistance R_{on} is given. Hence, conduction losses of both SiC switching devices will be smaller at any given operating point in this work.

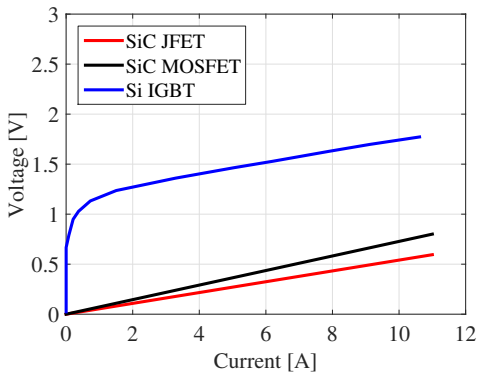

Fig. 2. Forward voltages of different switching devices at 25 °C junction temperature

E. Dynamic characteristics

Another benefit when using SiC devices are the reduced switching losses in a given converter application. In an initial design approach, switching energies are mostly compared based on the information provided in the datasheet. However, this may lead to unfair comparisons if the test setup differ from one manufacturer to another (use of different free-wheeling diodes with different reverse recovery currents, different gate resistors, etc.). Therefore, this work compares the switching energies at exactly the same test conditions including the same inductor and the same free-wheeling diode. Furthermore, the gate resistors are adjusted to maintain a similar peak gate current for a fair comparison. The test setup is shown in Fig. 3a and the current measurement (flat current shunt) is shown in Fig. 3b which has been presented in [28].

The gate-source/gate-emitter voltages are measured with a LeCroy PP011 voltage probe having a bandwidth of 500 MHz, the drain-source/collector-emitter voltages are measured with a 400 MHz LeCroy PPE4kV voltage probe. The voltage drop across the shunt resistor is measured with a LeCroy PP011 voltage probe as well which is then translated back to the current according to Ohm's law. The turn on switching transitions of all three devices are shown in Fig. 4. One can clearly see the superior switching performance of the two SiC switching devices compared to the Si IGBT. All waveforms are captured such that the gate turn on occurs at the same time. The SiC MOSFET and the SiC JFET show similar switching speeds. Where the SiC MOSFET has a lower di/dt compared to the SiC JFET, its dv/dt is higher. Hence similar turn on switching energies are expected for the MOSFET and the JFET.

The turn off switching transitions are shown in Fig. 5 in order to complete the dynamic performance comparison. Also during the turn off events, both SiC switching devices show much faster transitions than the IGBT. However, within the comparison of SiC devices, the MOSFET turns off quicker than the SiC JFET alternative. Maximum dv/dt and di/dt values for each switching device are shown in Table II in order to quantify the switching transitions. Having the voltage and

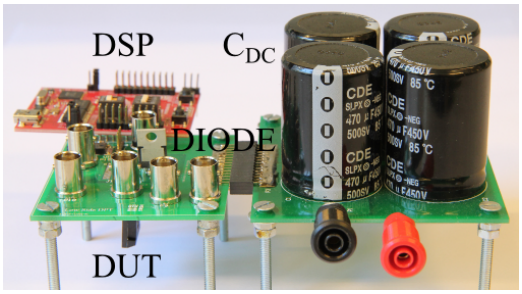

(a) Double pulse test setup

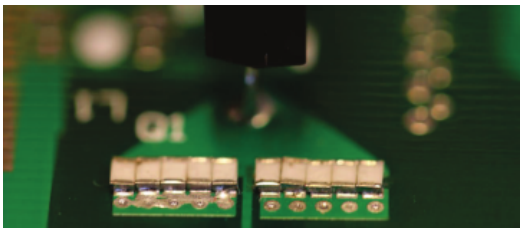

(b) Current measurement

Fig. 3. Double pulse test setup and current measurement

current measured on the oscilloscope, switching energies can then be obtained by numerically integrating the instantaneous power (which is simply the product of the measured voltage and current). The results of this procedure for currents from 2 A to 10 A are shown in Fig. 6. It verifies that the Si IGBT has highest switching energies for both turn on and turn off, though the discrepancy is larger at the turn off energies. That is mainly due to the tail current associated to Si IGBTs. Especially at larger currents, the SiC devices outperform the Si IGBT. Comparing the SiC switching devices, the SiC MOSFET shows lower turn off switching energies compared to its SiC JFET competitor at increased currents.

III. Boost Converter

Based on the previous analysis, the performance comparison between the SiC switching devices can be extended to a loss analysis for a given power converter; in this work it is a boost converter with specifications for a typical PV system whose block diagram is shown in Fig. 7a. The main components of the boost converter are the boost inductor L, the switching element S and a diode D as depicted in Fig. 7b. Assuming continuous conduction mode (CCM) with two different input voltages, 400 V and 500 V, and a fixed output voltage of 700 V, the duty cycle d can then be calculated according to

$$d = 1 - \frac{V_{in}}{V_{out}} \tag{3}$$

TABLE II
Switching Evaluation

	Turn on			Turn off		
	IGBT	MOSFET	JFET	IGBT	MOSFET	JFET
dv/dt in kV/µs	16	40	23	8	27	18
di/dt in kA/µs	0.5	1.1	3.3	0.06	0.3	0.2

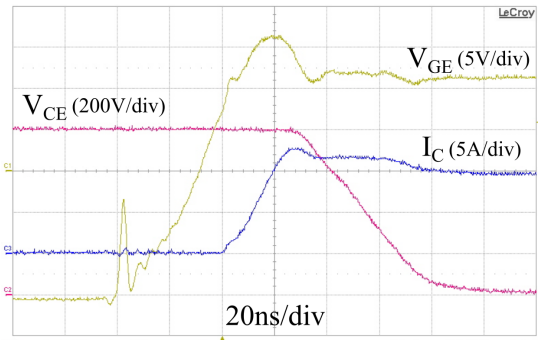

(a) Turn on IGBT, $R_g = 18\,\Omega$

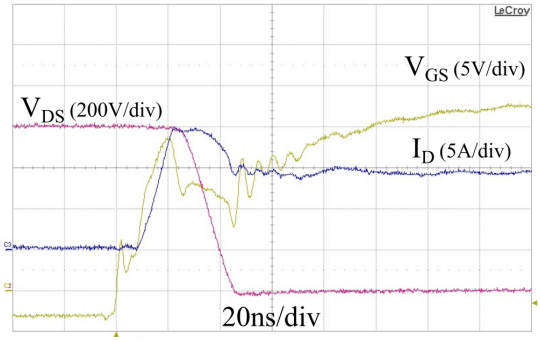

(b) Turn on MOSFET, $R_g = 18\,\Omega$

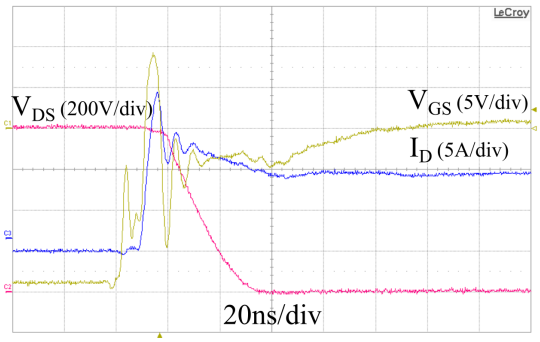

(c) Turn on JFET, $R_g = 10\,\Omega$

Fig. 4. Turn on transitions. $V_{DC} = 800$ V, $I = 10$ A

Maximum output power is set to 4 kW in this work to represent a residential PV system. The DC component of the current flowing through the boost inductor can then be calculated

$$I_{L\,DC} = \frac{V_{in} P_{out}}{(1-d)^2 V_{out}^2} \tag{4}$$

The current ripple is often a crucial factor when designing the boost converter as it creates harmonics and causes EMI. A typical design procedure is to limit the current ripple ΔI to be around 20 % of the DC current. With a switching frequency f_{sw} initially set to 20 kHz in order to avoid audible noise coming from the inductor, the size of the inductor is calculated to be 3 mH.

$$L = \frac{V_{in} d}{2 \Delta I f_{sw}} \tag{5}$$

This yields in a current ripple of 22 %. The 3 mH boost inductor is taken from a commercial PV inverter and it

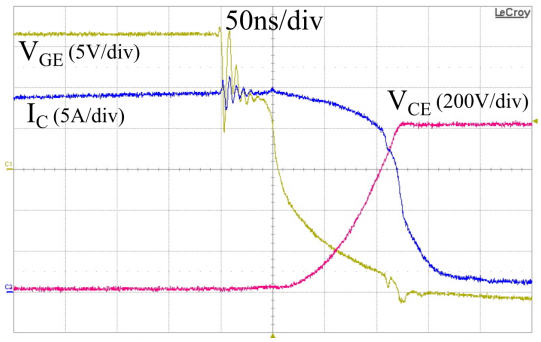

(a) Turn off IGBT, $R_g = 18\,\Omega$

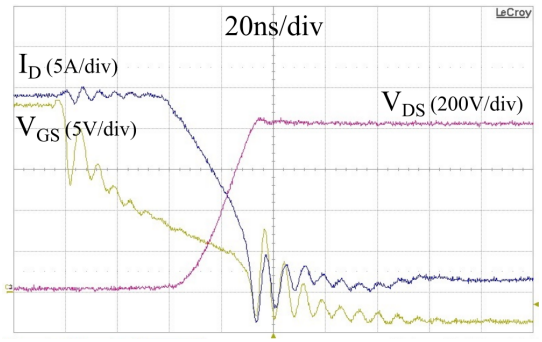

(b) Turn off MOSFET, $R_g = 18\,\Omega$

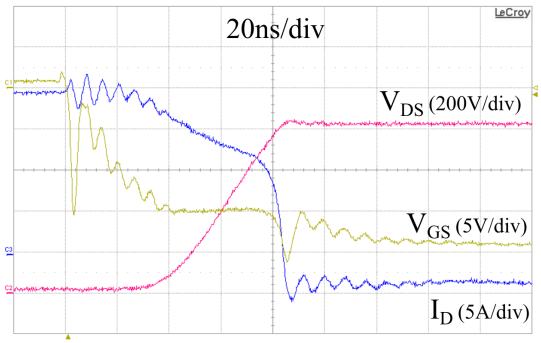

(c) Turn off JFET, $R_g = 10\,\Omega$

Fig. 5. Turn off transitions. $V_{DC} = 800\,\text{V}$, $I = 10\,\text{A}$

comprises of six KoolMu 77439-A7 cores stacked together with 60 turns. Taking advantage of the superior switching characteristics of the SiC switching devices, the switching frequency is increased to 100 kHz in this work which then reduces the size of the inductor for a given current ripple according to Eq. (5). The new inductor is set to 1 mH which will result in a current ripple percentage of 13 % only. This gives a current ripple decrease of more than 40 %. The new inductor is made of one MPP 55192-A2 core which in general may be more expensive than KoolMu, but it has a superior core loss performance which is very attractive at increased switching frequency operation. Also, due to the reduction in inductor size, only one core is necessary whereas the 3 mH core uses six KoolMu cores stacked together. Table III summarizes the most important specifications and Fig. 8 shows both inductors used in this work.

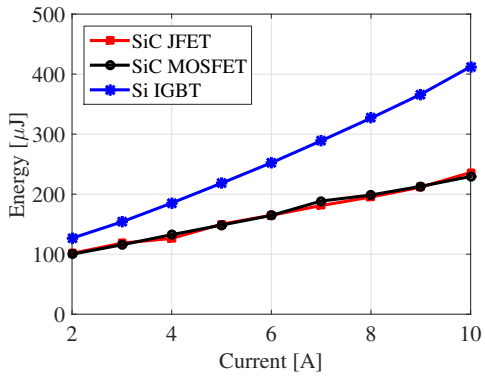

(a) Turn on energies

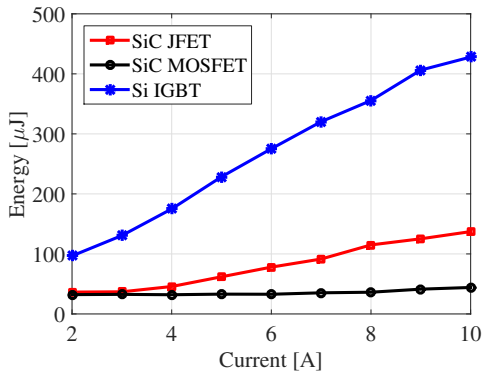

(b) Turn off energies

Fig. 6. Switching energy comparison of the three devices for different current levels. $V_{DC} = 800\,\text{V}$

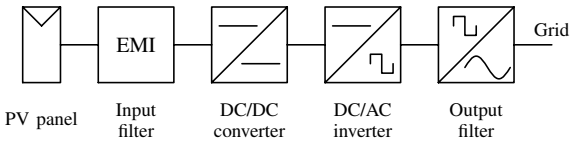

(a) Block diagram of a PV inverter system

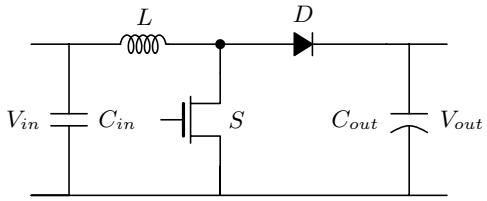

(b) Boost converter

Fig. 7. Block diagram of PV system in (a), schematic of a single phase boost converter in (b)

TABLE III
BOOST INDUCTOR PARAMETERS

	Inductor 1	Inductor 2
Inductance in [mH]	3	1
Cores	6xKoolMu 77439-A7	1xMPP 55192-A2
Turns	60	88
Volume in [cm^3]	345	72
Weight in [g]	1000	230

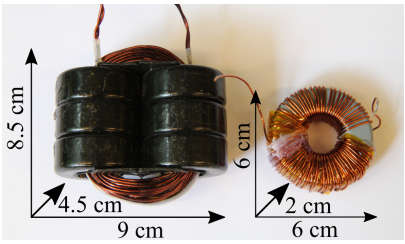

Fig. 8. Boost inductors used for different switching frequencies

A. Loss analysis

Since this work primarily compares the performances of the switching devices, the loss analysis focuses on the semiconductor losses only as this is where the loss reduction occurs. The conduction losses in the Si IGBT and the SiC diode can be expressed using piece-wise linear models, i.e.

$$P_{con Si,D_x} = V_f I_{AV} + r_{on} I^2_{rms} \tag{6}$$

where V_f represents the zero on-state voltage, I_{AV} the average current through the switching device, r_{on} the dynamic on-state resistance and I_{rms} the root-mean-square (RMS) value of the current through the switch. The SiC MOSFET and SiC JFET are unipolar devices and hence only the on-resistance $R_{DS(on)}$ is used to calculate the conduction losses,

$$P_{con SiC} = R_{DS(on)} I^2_{rms} \tag{7}$$

Referring to Fig. 6, the switching energies show a linear relationship to the current. Assuming the small ripple approximation, switching energies for a given base voltage ($V_{Base} = 800V$ in this work) can be described as

$$E_{on Si,SiC} = a_{on} I_{L DC} + b_{on} \tag{8}$$

$$E_{off Si,SiC} = a_{off} I_{L DC} + b_{off} \tag{9}$$

with a_{on},a_{off},b_{on} and b_{off} being the curve fitting constants. Switching losses can then be obtained by linear scaling the switching energies to the given switching voltage of the device (which is the output voltage in the case of a boost converter) and by multiplying the result with the chosen switching frequency f_{sw}

$$P_{sw} = f_{sw} \frac{V_{out}}{V_{Base}} \left(E_{on Si,SiC} + E_{off Si,SiC} \right) \tag{10}$$

Applying Eq. (6)-Eq. (10), the semiconductor losses can be calculated for any given operating point. As an example, for an output power of 2.5 kW and the two different input voltages (namely 400 V and 500 V), the results for the semiconductor loss breakdown analysis are shown in Fig. 9. The IGBT switching losses show a dominant contribution to the overall semiconductor losses. For instance, at an input voltage of 400 V, switching losses in the IGBT are 11.8 W whereas the switching losses of the SiC MOSFET are only 4.3 W which gives a switching loss reduction of more than 60 %. Not only switching loss reduction occurs by replacing the switching element to a SiC device. Also conduction losses

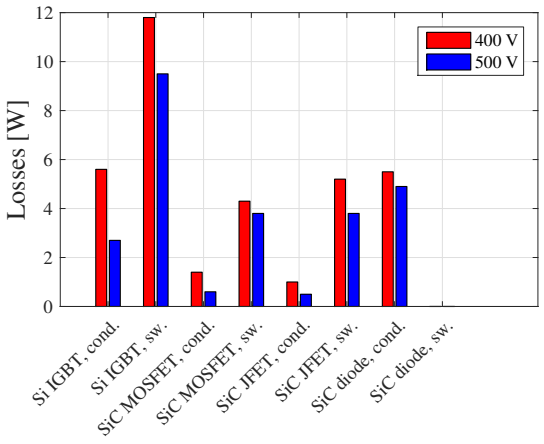

Fig. 9. Semiconductor loss breakdown analysis

can be drastically reduced. Taking an input voltage of 400 V as an example, conduction losses in the Si IGBT are 5.6 W and can be reduced down to 1.4 W with a SiC MOSFET. This gives a conduction loss reduction of 75 %. The diode contributes to the semiconductor losses with 5.5 W. A total semiconductor loss reduction of 11.7 W is achieved with the utilization of SiC MOSFETs for an input voltage of 400 V. Thus total semiconductor losses can be reduced by more than 50 %.

B. Experimental results

To verify the loss modeling approach from the previous section, a boost converter prototype is designed and shown in Fig. 10. Efficiencies for an output power up to 4 kW are recorded using a N4L PPA5500 power analyzer with a basic accuracy of 0.02 % and which can measure harmonics up to 2 MHz. The operating specifications are given in Table IV. Starting with a switching frequency of 20 kHz and 400 V input voltage, the results are shown in Fig. 11a and for an input voltage of 500 V, the results are presented in Fig. 11b. Both graphs show that both the Si and SiC based converters can achieve high efficiencies over 98 % throughout almost the entire operating range. Using SiC switching devices, maximum efficiency improvements of around 0.4 % can be achieved

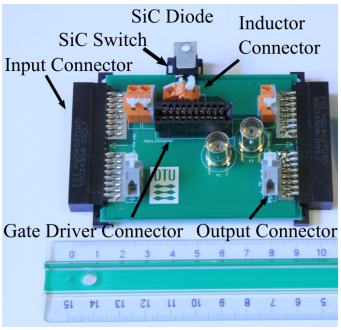

Fig. 10. Prototype of a 4 kW boost converter, heatsink not shown

TABLE IV
SPECIFICATIONS

Symbol	Meaning	Value
V_{in}	Input voltage	400 V to 500 V
V_{out}	Output voltage	700 V
f_{out}	Switching frequency	20 kHz, 100 kHz
L_{out}	Boost inductor	3 mH, 1 mH

which is a semiconductor loss reduction of more than 12 W. It is now possible to compare the predicted semiconductor loss reduction based on the modeling approach from the previous section with the measurements presented in this section. Fig. 12 shows that the predictions and measurements match well throughout the entire operating range. Furthermore, it states that the loss reduction with SiC based converters is greater at lower input voltages. The reason for that lies in the larger input current and duty cycle of the switch for a given output voltage and output power, which then stresses the switching element more because of the increased switched current (larger switching losses) combined with the larger conduction losses due to the larger RMS current through the switch.

Since the modeling approach from the previous section matches well with the measurements, the semiconductor loss models can be used with confidence for further analysis, presenting the semiconductor losses for the three switching devices in Fig. 13 in order to give a direct performance comparison. The increase in semiconductor losses against the output power is greatest for the IGBT whereas the MOSFET and the JFET show similar performance behavior. The reason for that is that the MOSFET has lower switching energies compared to the JFET, but its on-resistance is higher which,

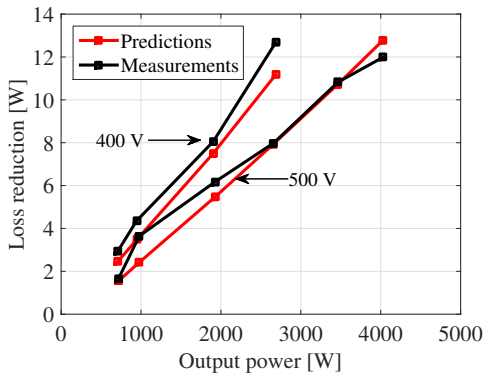

Fig. 12. Measured loss reduction versus predicted loss reduction. The comparison is based on the Si IGBT and the SiC JFET based converter

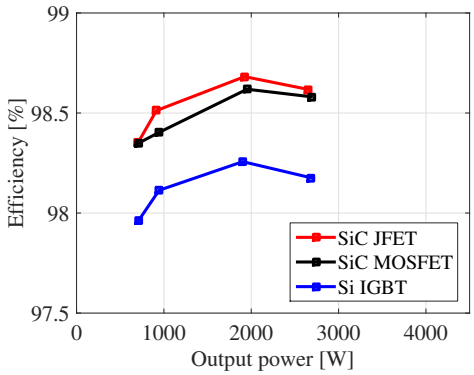

(a) Efficiencies for $V_{in} = 400$ V

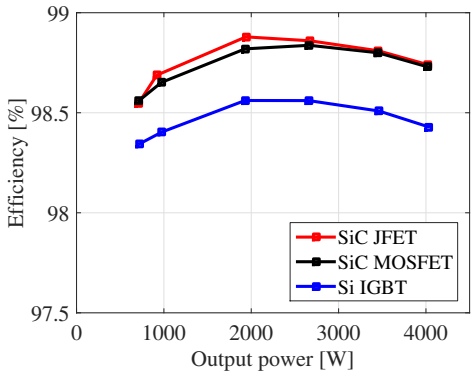

(b) Efficiencies for $V_{in} = 500$ V

Fig. 11. Efficiency measurements for a switching frequency of 20 kHz and an input voltage of 400 V in (a) and for an input voltage of 500 V in (b)

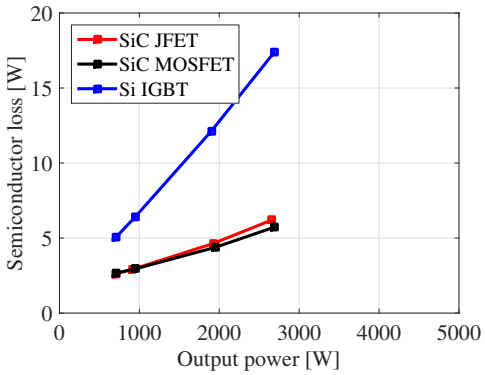

(a) Semiconductor loss for $V_{in} = 400$ V

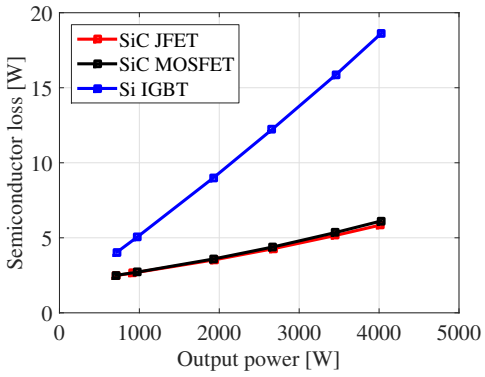

(b) Semiconductor loss for $V_{in} = 500$ V

Fig. 13. Semiconductor losses of the switching elements for different input voltages and output power

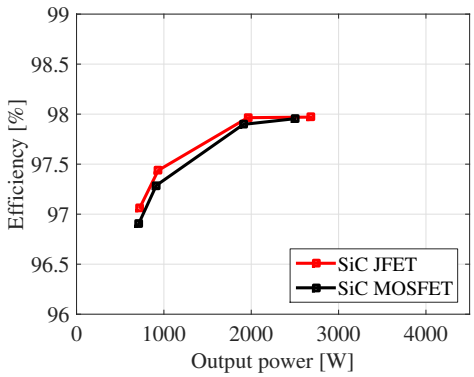

(a) Efficiencies for $V_{in} = 400\,\mathrm{V}$

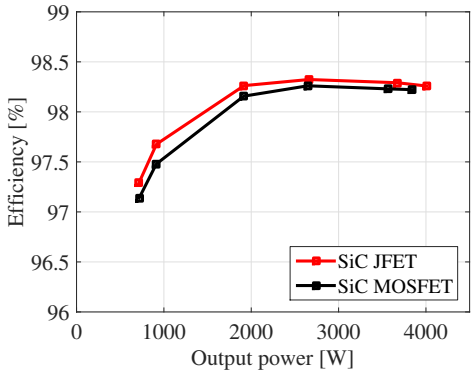

(b) Efficiencies for $V_{in} = 500\,\mathrm{V}$

Fig. 14. Efficiency measurements for a switching frequency of 100 kHz and an input voltage of 400 V in (a) and for an input voltage of 500 V in (b)

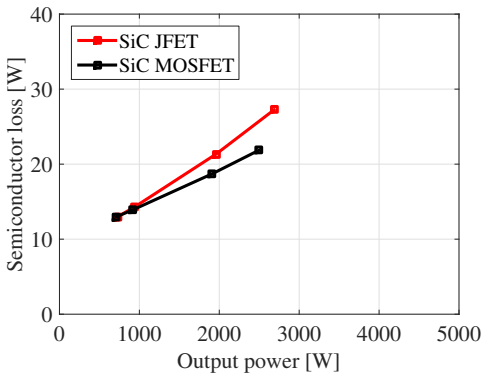

(a) Semiconductor loss for $V_{in} = 400\,\mathrm{V}$

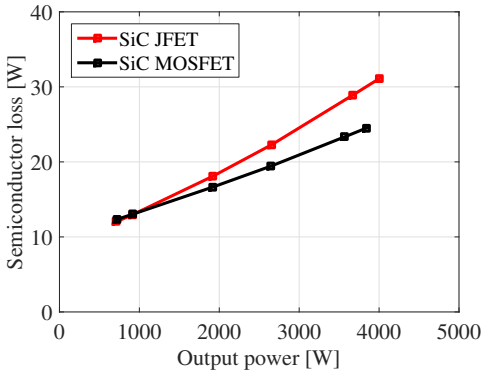

(b) Semiconductor loss for $V_{in} = 500\,\mathrm{V}$

Fig. 15. Semiconductor losses of the switching elements for different input voltages and output power

in the end, results in very similar total semiconductor losses throughout the entire operating range.

Using SiC switching devices for increased switching frequency operation, in order to reduce the size of the passive components measurements are repeated for 100 kHz operation with the 1 mH inductor. The results are shown in Fig. 14. Also at higher switching frequencies, efficiencies are still close to each other and a peak value of up to 98.3 % is achieved. Only at low power operation, a significant drop in efficiency is present mainly because the switching losses and the core losses are major contributions in that operating range. It is worthy of comment that the SiC JFET seems to have higher efficiencies especially in the lower power range. Referring to Fig. 6, the SiC JFET has quite competitive turn off switching energies to the SiC MOSFET at low currents and the difference becomes only significant as the current increases. However, as the current increases at increased output power, the JFET can benefit from its lower on-resistance. Therefore, instead of looking at the overall efficiencies, semiconductor losses are used (based on the modeling approach from the previous section), shown in Fig. 15. One can see that the semiconductor losses of the SiC MOSFET become slightly lower compared to the JFET - especially at increased power levels. That is due to the superior turn off energies of the MOSFET which outperform the lower conduction losses of the JFET at this particular switching frequency. From a semiconductor loss point of view, the SiC MOSFET has total losses of almost 22 W at 400 V input voltage whereas the JFET has around 26 W. However, such loss reduction of 4 W operating at 2.6 kW output power has only a minor influence on the overall efficiency. The same statement can be extended to the operation with 500 V input voltage and up to 4 kW output power. Hence for the given specifications in this work, both the JFET and the MOSFET perform very similar in terms of semiconductor losses.

IV. Conclusion

In this paper, three state of the art switching devices have been compared to each other. The comparison uses analytical semiconductor loss models based on conduction losses derived from datasheet information, and switching losses obtained via switching transition measurements. The loss models and hence the predicted semiconductor loss reduction with the use of SiC switching devices are verified using electrical power measurements in a boost converter operating under various conditions up to 4 kW. Both SiC based converters achieve high efficiencies of up to 98.8 % at a switching frequency of 20 kHz, which is 0.4 % higher than its Si alternative. At that operating frequency, both SiC alternatives perform very similar. With SiC switching devices utilized, operating

frequency is increased up to 100 kHz which reduces the boost inductance from 3 mH down to 1 mH. This not only reduces the current ripple from 22 % down to 13 %, but also reduces the size and weight of the inductor by over 75 %. Even at 100 kHz operation, competitive efficiencies of up to 98.3 % can be achieved and both SiC alternatives show similar semiconductor losses. Therefore, within the specifications in this work, one SiC switching device can not be favored over the other based on a loss point of view.

REFERENCES

[1] T. Kerekes, R. Teodorescu, P. Rodríguez, G. Vázquez, and E. Aldabas, "A new high-efficiency single-phase transformerless PV inverter topology," *IEEE Trans. Ind. Electron.*, vol. 58, no. 1, pp. 184–191, Jan 2011.

[2] D.-Y. Jung, Y.-H. Ji, S.-H. Park, Y.-C. Jung, and C.-Y. Won, "Interleaved soft-switching boost converter for photovoltaic power-generation system," *IEEE Trans. Power Electron.*, vol. 26, no. 4, pp. 1137–1145, April 2011.

[3] C.-M. Ho, H. Breuninger, S. Pettersson, G. Escobar, and F. Canales, "A comparative performance study of an interleaved boost converter using commercial si and SiC diodes for PV applications," *IEEE Trans. Power Electron.*, vol. 28, no. 1, pp. 289–299, Jan 2013.

[4] L. Balogh and R. Redl, "Power-factor correction with interleaved boost converters in continuous-inductor-current mode," in *Applied Power Electronics Conference and Exposition, 1993. APEC '93. Conference Proceedings 1993., Eighth Annual*, Mar 1993, pp. 168–174.

[5] D. Stephani, "Status, prospects and commercialization of sic power devices," in *Device Research Conference, 2001*, June 2001, pp. 14–.

[6] A. Elasser, M. Kheraluwala, M. Ghezzo, R. Steigerwald, N. Evers, J. Kretchmer, and T. Chow, "A comparative evaluation of new silicon carbide diodes and state-of-the-art silicon diodes for power electronic applications," *IEEE Trans. Ind. Appl.*, vol. 39, no. 4, pp. 915–921, July 2003.

[7] X. Yuan, S. Walder, and N. Oswald, "EMI generation characteristics of sic and si diodes: Influence of reverse-recovery characteristics," *IEEE Trans. Power Electron.*, vol. 30, no. 3, pp. 1131–1136, March 2015.

[8] F. Guédon, S. Singh, R. McMahon, and F. Udrea, "Boost converter with sic jfets: Comparison with coolmos and tests at elevated case temperature," *IEEE Trans. Power Electron.*, vol. 28, no. 4, pp. 1938–1945, April 2013.

[9] Y. Gao, A. Huang, S. Krishnaswami, J. Richmond, and A. Agarwal, "Comparison of static and switching characteristics of 1200 v 4h-sic bjt and 1200 v si-igbt," *IEEE Trans. Ind. Appl.*, vol. 44, no. 3, pp. 887–893, May 2008.

[10] N.-C. Sintamarean, F. Blaabjerg, H. Wang, and Y. Yang, "Real field mission profile oriented design of a SiC-based PV-inverter application," *IEEE Trans. Ind. Appl.*, vol. 50, no. 6, pp. 4082–4089, Nov 2014.

[11] H. Zhang, L. Tolbert, and B. Ozpineci, "Impact of SiC devices on hybrid electric and plug-in hybrid electric vehicles," *IEEE Trans. Ind. Appl.*, vol. 47, no. 2, pp. 912–921, March 2011.

[12] M. Swamy, K. Shirabe, and J. Kang, "Power loss, system efficiency, and leakage current comparison between si IGBT vfd and SiC FET vfd with various filtering options," *IEEE Trans. Ind. Appl.*, vol. PP, no. 99, pp. 1–1, 2015, early Access.

[13] F. Xu, B. Guo, L. Tolbert, F. Wang, and B. Blalock, "An all-sic three-phase buck rectifier for high-efficiency data center power supplies," *IEEE Trans. Ind. Appl.*, vol. 49, no. 6, pp. 2662–2673, Nov 2013.

[14] T. Friedli, S. Round, D. Hassler, and J. Kolar, "Design and performance of a 200-khz all-sic jfet current dc-link back-to-back converter," *IEEE Trans. Ind. Appl.*, vol. 45, no. 5, pp. 1868–1878, Sept 2009.

[15] H. Akagi, T. Yamagishi, N. Tan, S.-I. Kinouchi, Y. Miyazaki, and M. Koyama, "Power-loss breakdown of a 750-v 100-kw 20-khz bidirectional isolated dc-dc converter using sic-mosfet/sbd dual modules," *IEEE Trans. Ind. Appl.*, vol. 51, no. 1, pp. 420–428, Jan 2015.

[16] M. Treu, R. Rupp, P. Blaschitz, K. Ruschenschmidt, T. Sekinger, P. Friedrichs, R. Elpelt, and D. Peters, "Strategic considerations for unipolar sic switch options: Jfet vs. mosfet," in *Industry Applications Conference, 2007. 42nd IAS Annual Meeting. Conference Record of the 2007 IEEE*, Sept 2007, pp. 324–330.

[17] M. Treu, R. Rupp, and G. Sölkner, "Reliability of sic power devices and its influence on their commercialization - review, status, and remaining issues," in *Reliability Physics Symposium (IRPS), 2010 IEEE International*, May 2010, pp. 156–161.

[18] A. Lemmon, M. Mazzola, J. Gafford, and K. Speer, "Comparative analysis of commercially available silicon carbide transistors," in *Applied Power Electronics Conference and Exposition (APEC), 2012 Twenty-Seventh Annual IEEE*, Feb 2012, pp. 2509–2515.

[19] T.-T. Nguyen, A. Ahmed, T. Thang, and J.-H. Park, "Gate oxide reliability issues of sic mosfets under short-circuit operation," *IEEE Trans. Power Electron.*, vol. 30, no. 5, pp. 2445–2455, May 2015.

[20] R. Ouaida, M. Berthou, J. León, X. Perpiñà, S. Oge, P. Brosselard, and C. Joubert, "Gate oxide degradation of SiC MOSFET in switching conditions," *IEEE Electron Device Lett.*, vol. 35, no. 12, pp. 1284–1286, Dec 2014.

[21] X. Huang, G. Wang, Y. Li, A. Q. Huang, and B. Baliga, "Short-circuit capability of 1200v sic mosfet and jfet for fault protection," in *Applied Power Electronics Conference and Exposition (APEC), 2013 Twenty-Eighth Annual IEEE*, March 2013, pp. 197–200.

[22] R. Lai, F. Wang, R. Burgos, D. Boroyevich, D. Zhang, and P. Ning, "A shoot-through protection scheme for converters built with sic jfets," *IEEE Trans. Ind. Appl.*, vol. 46, no. 6, pp. 2495–2500, Nov 2010.

[23] D. Aggeler, F. Canales, J. Biela, and J. Kolar, "Dv/dt -control methods for the SiC JFET/si MOSFET cascode," *IEEE Trans. Power Electron.*, vol. 28, no. 8, pp. 4074–4082, Aug 2013.

[24] D. Domes and X. Zhang, "Cascode light - normally-on jfet stand alone performance in a normally-off cascode circuit," in *PCIM Europe 2010; International Exhibition and Conference for Power Electronics, Intelligent Motion, Renewable Energy and Energy Management; Proceedings of*, May 2010.

[25] R. Siemieniec and U. Kirchner, "The 1200v direct-driven sic jfet power switch," in *Power Electronics and Applications (EPE 2011), Proceedings of the 2011-14th European Conference on*, Aug 2011, pp. 1–10.

[26] C. DiMarino, Z. Chen, D. Boroyevich, R. Burgos, and P. Mattavelli, "Characterization and comparison of 1.2 kv sic power semiconductor devices," in *Power Electronics and Applications (EPE), 2013 15th European Conference on*, Sept 2013, pp. 1–10.

[27] S. Round, M. Heldwein, J. Kolar, I. Hofsajer, and P. Friedrichs, "A sic jfet driver for a 5 kw, 150 khz three-phase pwm converter," in *Industry Applications Conference, 2005. Fourtieth IAS Annual Meeting. Conference Record of the 2005*, vol. 1, Oct 2005, pp. 410–416 Vol. 1.

[28] A. Anthon, J. Hernandez, Z. Zhang, and M. Andersen, "Switching investigations on a sic mosfet in a TO-247 package," in *Industrial Electronics Society, IECON 2014 - 40th Annual Conference of the IEEE*, Oct 2014, pp. 1854–1860.